





Article

# A Novel Methodology for Adaptive Coordination of Multiple Controllers in Electrical Grids

Ruben Tapia-Olvera <sup>1</sup>, Francisco Beltran-Carbajal <sup>2</sup>, Antonio Valderrabano-Gonzalez <sup>3,\*</sup> and Omar Aguilar-Mejia <sup>4</sup>

<sup>1</sup> Department of Electrical Energy, Universidad Nacional Autónoma de México, Mexico City 04510, Mexico; rtapia@fi-b.unam.mx

<sup>2</sup> Department of Energy, Universidad Autónoma Metropolitana, Unidad Azcapotzalco, Mexico City 02200, Mexico; fbeltran@azc.uam.mx

<sup>3</sup> Facultad de Ingeniería, Universidad Panamericana, Álvaro del Portillo 49, Zapopan 45010, Mexico

<sup>4</sup> School Engineering, UPAEP University, Puebla 72410, Mexico; omar.aguilar@upaep.mx

\* Correspondence: avalder@up.edu.mx

**Abstract:** This proposal is aimed to overcome the problem that arises when diverse regulation devices and controlling strategies are involved in electric power systems regulation design. When new devices are included in electric power system after the topology and regulation goals were defined, a new design stage is generally needed to obtain the desired outputs. Moreover, if the initial design is based on a linearized model around an equilibrium point, the new conditions might degrade the whole performance of the system. Our proposal demonstrates that the power system performance can be guaranteed with one design stage when an adequate adaptive scheme is updating some critic controllers' gains. For large-scale power systems, this feature is illustrated with the use of time domain simulations, showing the dynamic behavior of the significant variables. The transient response is enhanced in terms of maximum overshoot and settling time. This is demonstrated using the deviation between the behavior of some important variables with StatCom, but without or with PSS. A B-Spline neural networks algorithm is used to define the best controllers' gains to efficiently attenuate low frequency oscillations when a short circuit event is presented. This strategy avoids the parameters and power system model dependency; only a dataset of typical variable measurements is required to achieve the expected behavior. The inclusion of PSS and StatCom with positive interaction, enhances the dynamic performance of the system while illustrating the ability of the strategy in adding different controllers in only one design stage.



**Citation:** Tapia-Olvera, R.; Beltran-Carbajal, F.; Valderrabano-Gonzalez, A.; Aguilar-Mejia, O. A Novel Methodology for Adaptive Coordination of Multiple Controllers in Electrical Grids. *Mathematics* **2021**, *9*, 1474. <https://doi.org/10.3390/math9131474>

Academic Editor: Cristina I. Muresan

Received: 19 May 2021

Accepted: 15 June 2021

Published: 23 June 2021

**Publisher's Note:** MDPI stays neutral with regard to jurisdictional claims in published maps and institutional affiliations.



**Copyright:** © 2021 by the authors. Licensee MDPI, Basel, Switzerland. This article is an open access article distributed under the terms and conditions of the Creative Commons Attribution (CC BY) license (<https://creativecommons.org/licenses/by/4.0/>).

**Keywords:** B-spline neural networks; adaptive power system control; coordinated multiple controllers; StatCom

## 1. Introduction

Electric power systems are large, interconnected, complex, and highly changeable systems that are always affected by a wide variety of perturbations [1]. Therefore, the control design stage and tuning procedure for multiple controllers is an entangled task [2,3], present interesting approaches on stabilizing procedures in electric power systems that use multiple power system stabilizers with lead and lag compensators. The conventional linear controllers designed around an equilibrium point are useful, but their performance could be degraded if variations are presented in the system. On the other hand, dealing with non-linear controllers is a high demanding and slow task due to the complexity of large-scale power system. In general, for reaching a good performance, these strategies present dependency on the parameters system modeling.

Power system stabilizers (PSS) have been used to generate supplementary signals to control the excitation system to improve the power system dynamic performance by the damping of system oscillations [1]. However, the expected behavior depends entirely on

the correct selection of controllers' gains and time constants [2,3]. Moreover, some flexible alternating current transmission systems (FACTS devices) are included to solve some specific power systems problems; nevertheless, their operation is also depending upon the positive interaction with other regulation devices. Refs. [4,5] exemplify the problem of simultaneous tuning of multiple controllers in large scale power system including FACTS devices in transmission systems.

There are several methodologies to solve the problem of designing linear controllers to reach good dynamic performance. However, these solutions are complex in implementation; they do not cover a wide range of operating conditions of the power system or they do not have the same behavior with new grid topologies. The main objective of this proposal is to attain an adaptive performance of PSS in large-scale power systems with the possibility of adding new components that change the grid configuration, in this case for exemplifying through a static synchronous compensator (StatCom).

In order to validate the proposed strategy and without loss of generality, this paper presents the control design problem of PSS in power systems including a StatCom, which is one of the most useful FACTS devices in practical power systems. This configuration adds enough complexity to verify the viability of the proposal.

In general, the design control stage has been considered an independent problem, with only one controller. The fact that the system can have other regulation devices, has not been included. Only few works contemplate more than one controller simultaneously in the design stage. However, this is an open research topic due to the electrical grid composition and the continuous topology changing on it [6].

In [2] two objective functions must be solved to obtain coordination between PSS and traditional static VAR compensators (SVC). In order to reduce the high computational load, the genetic algorithm was used for solving the multi-objective optimization problem, adapting it for parallel computing. An analysis based on the power system modeled as a set of hybrid non-linear differential algebraic equations is presented in [3], where the dynamic behavior of the system is studied in various scenarios: no PSS, PSS without dead-band, and PSS with dead-band.

In [7], a single machine infinite bus (SMIB) model is used to tune the PSS, and then new non-specified adjustments are carried out to extend the scheme to the multimachine scenario. Additionally, the tuning stage is very case-dependent. Multi-band PSS are tuned in [8] by using an optimization search method based on modal performance index, but representative linearized system models are required for the optimization procedure.

The PSS tuning based on linear quadratic regulator design is presented in [9]. The state and input matrices of the linearized power system model are required for developing the optimization procedure in a single machine case, and then it is extended to the multi-machine case. In [10], a two-level control strategy that blends a local controller with a centralized controller is proposed to diminish low frequency oscillations. In the PSS model, a proportional integral (PI) controller is added. Two extra gains are included in the problem solution. For the tuning procedure, two stages are required, first the design of the local PI controller and then the design of the centralized controller.

A design method using a modified Nyquist diagram with an embedded partial pole-placement capability is presented in [11]. The small signal stability model obtained by the linearization of the power system around an operating point is required. That method evaluates the open loop transfer function along a line of constant damping ratio to design PSS for two test systems.

Additionally, control design based on non-linear theory is used, but in the same sense the procedure is realized separately for each controller. In [12], a scheme called decentralized continuous higher-order sliding mode excitation control is applied. The deviations on the angle of the power are required to obtain the desired system performance, also the estimation of first and second order time derivatives of this angle must be determined. Similarly, in [13] the  $H_\infty$  control with regional pole placement is used to ensure adequate power system dynamic performance, the linearized model around an equilibrium point

is also needed. Additionally, deterministic strategies based on artificial intelligence could be an alternative to the design procedure of multiple controllers in electrical grids [14]. Another important algorithm is the non-linear feed forward control which represents an option of non-linear adaptive control techniques [15]. This kind of strategies has been little explored in applications for electrical power systems. Similarly, other approach that can be extended to large scale power systems is the physics-based control technique [16].

A scheme called networked predictive control (NPC) used to design a damping controller that incorporates a generalized predictive control (GPC) to generate optimal control predictions is presented in [17]. Model identification is required to deal with uncertainties and to provide an adaptive predictive model for GPC. This method describes four steps for designing a NPC for a wide area damping controller: (i) modal analysis of the detailed non-linear model; (ii) determination of the order of the reduced order model of the power system; (iii) obtain the low-order equivalent model via model identification algorithm and use it as the prediction model for the NPC; (iv) selection of parameters like the output prediction horizon, the control horizon, the weighting sequence, and the sampling period.

Finally, artificial intelligence methodologies such as artificial neural networks (ANN), fuzzy logic (FL), or neuro-fuzzy are used for design purposes. In [18] an adaptive fuzzy sliding mode controller with a PI switching surface to damp power system oscillations is proposed. This strategy combines: (a) a sliding surface, (b) a fuzzy controller, (c) a curbing controller, and (d) a wavelet neural network to obtain the best auxiliary signal input to the excitation system. The structure of wavelet neural network is based on three layers, where the inputs are the sliding surface and its derivative.

A so-called hybrid adaptive non-linear controller is proposed in [19]. For the controller design it is necessary to estimate non-linear parts of the system, it is also required to measure data. The controller has a feed forward neural network structure, it is trained offline with extensive test data and it is adjusted online. In [20], the design of a PSS based on a combination of fuzzy logic and sliding mode theory is illustrated. This proposal indicates that a fuzzy-PID controller is composed of fuzzy PI and fuzzy PD controllers, and the response depends on scaling factors, hence selection of these parameters is crucial while designing the controller. The definition of the fuzzy rules is also an important issue for its correct operation.

Other important proposals, including FACTS devices, offer better results working with positive interaction with PSS. In [4], an optimization formulation is used to coordinate one PSS with one unified power flow controller (UPFC), but two objective functions based on eigenvalues of the state are needed for it. The possibility of using different FACTS devices is indicated in [5], the results include a StatCom and a UPFC. The eigenvalues of the power system model are required on the tuning procedure.

In [21], a StatCom and a PSS have been tuned to get a good dynamic power system performance using the seeker optimization algorithm to obtain the controller gains by an objective function. The StatCom model used, includes the components of the current and voltage dynamic in terminals of direct current (DC) capacitor.

Similarly, an objective function in [22] is used to attain a positive interaction between StatCom and PSS with a constraint set. The StatCom model is described with the operating range curve, but no dynamic equations are included. In [23], the dynamic operation of the StatCom is coordinated with a PSS. The tuning procedure depends on an objective function, and the definition of a constrain set.

The changing nature of power systems demands different types of studies due the inclusion of new control devices, renewable energies, and emerging technologies. However, it is difficult to have a unique methodology to solve the problem of the control design in large-scale power system. Although there are different alternatives to solve this problem, these proposals offer a solution limited to the characteristics of the systems under study. In multimachine power systems the control design problem is amplified due to the presence

of multiple controllers that must be tuned simultaneously to guarantee a positive interaction for each operating condition.

Therefore, the present contribution considers the non-linear power system nature and it defines an adaptive controllers' behavior. This performance is obtained by the inclusion of some selected dynamic gains that are updated on each sample time to find the best values for every operating condition and system topology. It is possible to update all the controller gains, but to exemplify the relevance of the proposal, only some of them are dynamically calculated. Simultaneous tuning of each controller is obtained.

To validate the proposed scheme based on B-Spline neural networks, PSS are simultaneously coordinated with a StatCom to enhance the power system dynamic response under severe disturbances. An effective control design procedure for power system controllers is demonstrated by the obtained results, improving the overall multimachine system dynamic performance. The proposal avoids the parameters and power system model dependency by using only measurements of some system variables to reach the expected behavior. The main contributions of our methodology are: (i) a new method for tuning multiple controllers in electrical grids is proposed; (ii) a time-domain analysis for damping low frequency oscillations considering different controllers when previous design stage was already performed is included; (iii) different controllers preserving good performance without imposing a particular requirement are considered; (iv) the introduced methodology offers a practical way to obtain adaptive behavior of controllers with simultaneously tuning, and positive interaction; (v) the proposed algorithm is learning online, which means no additional stages for training are required.

## 2. Electric Grid Operation and Control

Transient stability in large-scale power system is usually demonstrated by time domain simulations over a range of operating conditions and perturbations due to the complexity to dealing with large non-linear models associated to the power systems. Typically, the most demanding scenarios are first analyzed to have the power system with good dynamic performance, and then, similar or better behavior is expected when less demand occurs.

On the other hand, the classical stability analysis based on the power system linearized model has high complexity to attain an accurate linearized model, moreover, new components integration, and the consideration of continuous grid change involves new equilibrium points. These aspects represent another important open research topic.

Thus, we used a complete non-linear representation for transient stability studies in large-scale power system. Besides that, our proposal is proved under three phase faults, which are considered severe disturbances. The solution under these considerations is gotten by numerical methods involving a set of non-linear differential equations modeling all grid components with dynamic behavior.

Some models available in the literature are used to evaluate the proposed strategy. Additionally, the steady state condition and dynamic performance of the power system with excitation is developed in PSS<sup>®</sup> E. The results gotten are consistent in our simulation platform and the commercial software.

### 2.1. Power System Model

For transient stability studies, a synchronous generator model with four state variables  $\delta_i$ ,  $\omega_i$ ,  $E'_{qi}$ ,  $E'_{di}$ , and an automatic voltage regulator represented by a state variable  $E_{fdi}$  [1,24] is used Equation (1). Where subscript  $i$  identifies the  $i$ th generator. Then,

$$\begin{aligned}
\frac{d\delta_i}{dt} &= \omega_i - \omega_B \\
\frac{d\omega_i}{dt} &= \frac{\omega_B}{2H_i} [-D(\omega_i - \omega_B) + P_{mi} - P_{ei}] \\
\frac{dE'_{qi}}{dt} &= \frac{1}{T'_{d0i}} [-E'_{qi} + (x_{di} - x'_{di})i_{di} + E_{fdi}] \\
\frac{dE'_{di}}{dt} &= \frac{1}{T'_{q0i}} [-E'_{di} - (x_{qi} - x'_{qi})i_{qi}]
\end{aligned} \tag{1}$$

where  $\delta$  is the load angle;  $\omega$  is the angular speed;  $E'_q$  and  $E'_d$  are the quadrature and direct internal transient voltages, respectively;  $P_e$  is the injected real power;  $i_q$  and  $i_d$  are the quadrature and direct axis currents, respectively;  $E_{fd}$  is the excitation voltage;  $\omega_B$  is the speed in steady state condition;  $H$  is the inertia constant;  $T'_{d0}$  and  $T'_{q0}$  are the  $d$  and  $q$  open-circuit transient time constants;  $x'_d$  and  $x'_q$  are the  $d$  and  $q$  transient reactances;  $x_d$  and  $x_q$  are the  $d$  and  $q$  synchronous reactances;  $D$  is the damping constant. Considering this representation, the real power is obtained by,

$$P_{ei} = E'_{di}i_{di} + E'_{qi}i_{qi} + (x'_{di} - x'_{qi})i_{di}i_{qi} \tag{2}$$

This set of equations is solved along with the algebraic equations of the electric grid. The initial values of  $dq$ -axis currents are obtained by power flow analysis. The algebraic equations of the power grid are formulated by power flow representation and solved together with synchronous generator equations [24]. Additionally, a static excitation system is considered to regulate the terminal voltage in each equivalent model of synchronous generators,

$$\frac{dE_{fdi}}{dt} = \frac{1}{T_{Ai}} [-E_{fdi} + K_{Ai}(V_{refi} - V_{ti} + V_{si})] \tag{3}$$

where  $V_{ref}$  is the reference voltage;  $V_t$  is the terminal voltage magnitude;  $V_s$  is the PSS's output signal (auxiliary signal);  $K_A$  and  $T_A$  are the system excitation gain and time constant.

The power system stabilizer model has the representation by phase lag-lead compensators and a washout block. The error between the actual speed and the corresponding in steady state condition is considered as the input signal,  $\omega_i(s) - \omega_B$ . This auxiliary control signal,  $V_s$ , must guarantee a faster damping of the low frequency oscillations that occur in the system after a short circuit failure is presented. For this purpose, it is necessary to define properly:  $K_s$ ,  $T_w$ ,  $T_1$ ,  $T_2$ ,  $T_3$  y  $T_4$ , for each PSS included in the power system. In general, it is considered that  $T_1 = T_3$  y  $T_2 = T_4$ .

In Figure 1, the proposed adaptive scheme is included in the power system stabilizer model to attain improved dynamic performance. This non-linear model is used to validate the tuning on the proposal. The Equations (1)–(3) are not used for design purposes. The time response of some variables is used to train the adaptive scheme in offline stage and then also in online learning operation.

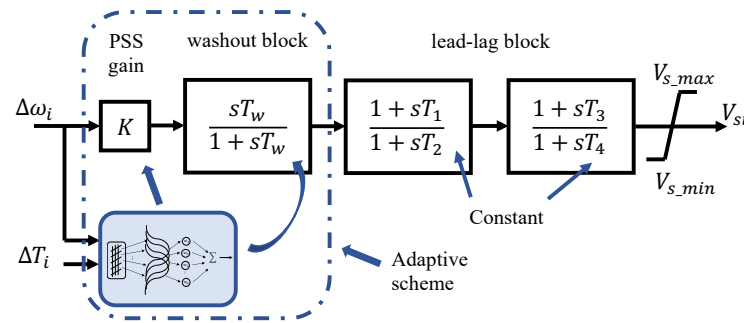


Figure 1. Improved power system stabilizers with adaptive scheme.

2.2. Statcom Model and Control

The StatCom model used on this paper consists of an equivalent transformer that emulates the voltage source converter operation. This transformer is connected in one side to a capacitor bank and, on the other side to the electric grid through a coupling transformer [25], Figure 2. One important feature of this model is the possibility to be included in transient stability studies of the power systems. The internal AC voltage of the StatCom is defined by,

$$V_{int} = km_a E_{dc} e^{j\phi} \tag{4}$$

where  $k$  is a known constant;  $E_{dc}$  is the DC voltage on the capacitor terminals;  $\phi$  is the phase angle of  $V_{int}$  in phasor form, and;  $m_a$  in this model emulated the index modulation to regulate the voltage magnitude.

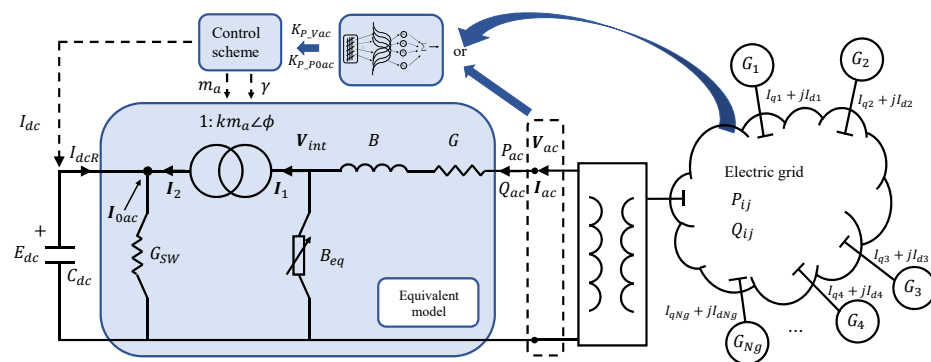


Figure 2. StatCom model with dynamic control gains.

Three PI controllers are used to regulate the StatCom dynamic performance, the main objective is to control the voltage magnitude at the point of common coupling (PCC), but an auxiliary signal could be included. In this scheme, the controlled voltage is after internal losses of the VSC,  $V_{ac}$ , before the PCC transformer. The real and reactive power of the presented equivalent circuit is defined by [25],

$$\begin{aligned} P_{ac} &= V_{ac}^2 G - km_a V_{ac} E_{dc} [G \cos \gamma + B \sin \gamma] \\ Q_{ac} &= -V_{ac}^2 B - km_a V_{ac} E_{dc} [G \sin \gamma - B \cos \gamma] \end{aligned} \tag{5}$$

where  $\gamma = \theta_{ac} - \phi$ , represents the angular aperture between the internal voltage of VSC model and terminals, after internal losses,  $G$  and  $B$ . This angle is the second control variable to guarantee the desired exchange of active power, in this case only the required active power from the grid for losses compensation of the StatCom,  $G$  and  $G_{sw}$ , the last one represents the switching losses. These power flow equations are solved together with the electrical grid.

The dynamic performance is evaluated by the resulting equations of the equivalent circuit in Figure 2. In the DC bus,

$$i_c = C_{dc} \dot{E}_{dc} \quad (6)$$

where  $i_c = -I_{dcR} - I_{dc}$ , also,

$$I_{dcR} = \frac{P_{0ac}}{E_{dc}} \quad (7)$$

where  $I_{dc}$  is the output of the first PI controller with  $E_{dc} - E_{dc}^{nom}$  as its input. Two controller gains,  $K_{P_{E_{dc}}}$  and  $K_{I_{E_{dc}}}$  are needed.

The capacitor cannot inject active power, so it is necessary one regulator to guarantee the physical condition that only active power losses are absorbed from the grid. Therefore, a second PI controller is employed for this task, where the input is  $P_{0ac}$  and the output is  $\gamma$ ,  $K_{P_{P_{0ac}}}$ , and  $K_{I_{P_{0ac}}}$  are needed.

Finally, a deviation from the nominal value (initial condition),  $m_a$ , is calculated by a third PI controller. This deviation helps to regulate  $V_{ac}$ . The adaptive PI controller input is defined as the difference between the desired and actual voltage magnitude,  $V_{ac} - V_{ac}^*$ ; also, two gain values must be properly specified for the StatCom connected to the electric grid,  $K_{P_{V_{ac}}}$  and  $K_{I_{V_{ac}}}$ . In total, six gains must be defined for the StatCom controllers. This model captures the main behavior in steady state and dynamic performance of the StatCom. Different to other models presented in the literature for this device, this model includes a phase-shifting transformer and an equivalent shunt susceptance, resulting in an explicit representation of the voltage source converter (VSC) in both sides the AC and DC, respectively. The reader interested in reviewing more details of this model can consult [25].

### 3. Dynamic Controllers' Gains

In some power systems, a low damping ratio is exhibited. Therefore, the tuning procedure of each controller is a task of precision; moreover, if several gains must be defined, a critical control design stage is presented. An alternative solution for this scenario is to analyze any steady-state condition, and then some gains could be updated online to attain better dynamic performance.

With our strategy it is possible to update all controllers' gains but, to exemplify the relevance of the proposal only some of them are dynamically calculated: the gains for the StatCom  $K_{P_{V_{ac}}}$  and  $K_{P_{P_{0ac}}}$  and for each PSS,  $K_s$  and  $T_w$ . A similar behavior in practice is expected, where only some of them could be retuned by an online procedure. Table 1 exhibits the main steps in proposed control design procedure. The first step consists in use typical gain values obtained around the steady state condition, which are present in Table 2 for the StatCom, and in Table 3 for the generators.

**Table 1.** Main stages in the proposed procedure to attain adaptive controllers.

Offline and Online Steps in the Proposed Methodology	
<b>(i) Offline stage</b>	<p>Extracted key signals from any steady state condition of the power system, input output mapping.</p> <p>Controllers are initialized to attain this equilibrium point.</p> <p>An initial architecture of neural networks is defined (shape, size, and learning rate).</p> <p>An accuracy neural networks architecture is obtained by training procedure, initial dataset.</p> <p>The proposal is test to different power system scenarios.</p>
<b>(ii) Online stage</b>	<p>The proposed algorithm is updating the controller gains if it required.</p> <p>The adaptive controllers follow new steady state power system condition.</p> <p>If disturbances are presented fast changes in controllers gains are exhibited.</p> <p>Several controllers are tuning simultaneously with positive interaction.</p>

Table 1. Cont.

Offline and Online Steps in the Proposed Methodology	
<b>(iii) New controllers</b>	
If new regulation strategies are included, the adaptive controllers update their self by online learning Equation (11).	
Additionally, if it has critic gains, it is possible include new neural networks schemes with a similar architecture, Figure 3.	

Table 2. Gains of StatCom controller.

Parameter	Value
$K_{PEdc}$	1
$K_{IEdc}$	1.5
$K_{Ip0ac}$	0.0015
$K_{Ivac}$	0.2
$R_{Itc}$	0 pu
$X_{Itc}$	0.05
$R_{VSC}$	$2 \times 10^{-3}$
$X_{VSC}$	0.01
$G_0$	$2 \times 10^{-3}$

Table 3. Gains of Generator controller.

Generator	$K_s$	$T_w$
1	91	10
2	97	9.8
3	100	10
4	100	10

The proposed adaptive PI controller in the StatCom scheme is defined by,

$$\begin{aligned} u(t) &= K_P(e_1)e(t) + K_I(e_1)x_{aux} \\ \dot{u}(t) &= e(t) \end{aligned} \tag{8}$$

For controlling purposes,  $K_P$  and  $K_I$  and the PSS constants must be defined adequately. We propose to update these gains using the adaptive control law of Figure 3, defined as Equation (9).

$$K_1(e_1) = \beta_1(e_1)\hat{W}_1^T \tag{9}$$

$K_1$  on the Equation (9), and Figure 3 is used for any of the gains to be calculated.

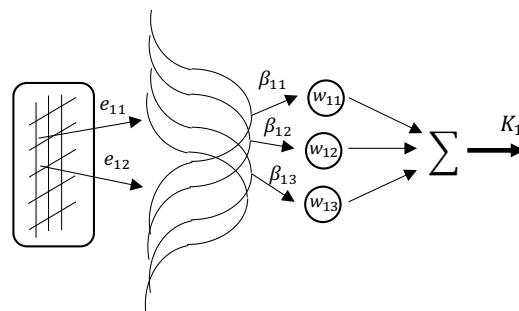


Figure 3. Schematic representation of update procedure.



$|e_1| \leq e^*$  with  $e^*$  being a constant. The update law for  $\hat{W}_1$  is given by,

$$\hat{W}_1 = W_1 + \Gamma_1(e_1, \beta_1, \zeta) \quad (10)$$

$\zeta \in \mathbb{R}$  is a positive constant;  $W_1 \in \mathbb{R}^P$  with positive constants and;  $\Gamma_1 \in \mathbb{R}^P$  calculated by

$$\Gamma_1 = -\frac{\zeta \beta_1}{\|\beta_1\|^2} e_1 \quad (11)$$

$\beta_1 \in \mathbb{R}^P$  represents a non-linear relationship from the input signals,  $e_1$ . The non-linear relationship is defined by polynomial splines, B-splines [26,27], in this paper are univariate B-spline of fourth order.

Therefore, the controllers update their performance on each sample time with Equations (9)–(11). The input space is normalized in such a way that the input error is bounded in magnitude. First the system is operating offline where learning ratio,  $\zeta$ , is defined in order to get the best performance [28,29]. Then, the dynamic gains are updated by Equation (11) and put to operate online. The results under this last condition are exhibited in Section 4.

The search begins with some typical known values of each gain Equation (12), then the training algorithm is developed to improve the dynamic system response.

$$\begin{aligned} K_{Pp0ac} &= 0.002 \\ K_{Pvac} &= 5 \\ T_1 = T_3 &= 0.05 \\ T_2 = T_4 &= 0.01 \\ V_{min} &\leq V_s \leq V_{max} \\ V_{max} = 0.05; V_{min} &= -0.05 \end{aligned} \quad (12)$$

After that, with each operating condition the adaptive algorithm continues learning with input variables and finding the best set of controller gains. The input signals for updating PSS gains are defined by,

$$e_{11} = \omega_i(t) - \omega_B \quad (13)$$

$$e_{12} = P_m - P_e(t) \quad (14)$$

The gains for the StatCom controller have only one input signal, defined by Equation (13). The online procedure consists in calculating the best value for each dynamic gain for the power system operative point. This is possible because the BSNN is updating the weighting vector as a result of input error modification.

Finally, the implementation of the B-Spline neural networks stepwise rules are presented in Table 4, where all mathematical details behind this approach are included.

In this work, B-Spline neural networks algorithm was selected because it requires less computational effort, thanks to its single layer of neurons, its structure, and the shape of the base functions, Figure 3, in contrast to the multi-layer neural networks architecture. Furthermore, the activation functions are linear with respect to the adaptive weights, with an instant learning rule that can be used to update and adjust the weights online. These conditions make the B-Spline neural networks algorithm able of modeling and regulating complex non-linear systems. With these features, a robust, optimal control system is obtained with the ability to be adapted to inherent non-linearities and external or internal disturbances of the system. One of the core aspects of selecting the use of the BSNN is that by defining the base functions a non-linear relation of the input is obtained, and the training algorithm is computationally efficient, with a numerically stable recurring relationship that works with any distribution of knot vector.

**Table 4.** 1: B-Spline Neural Network off-line training rules.

Input Define:	space lattice with n knot-vectors
Define:	basis functions (K order, shape and distribution)
Define:	number of knot-vector
Define:	nodes of hidden layer
	Define: Initial conditions (weights)
	Define: error signal and minimum and maximum values
	Define: threshold error
	while t < simulation time do
	Calculate the input and output value of each layer
	Calculate the errors between target and current value
	Includes several operating conditions
	if $e_x < \text{threshold error}$
	NN is ready for online operation
	return weights
	else
	Update weights
	Calculate the input and output value of each layer
	Calculate the errors between target and actual value
	if $e_x < \text{threshold error}$
	NN is ready for online operation
	return weights
	else
	Update weights
	Change data source and update learning rate
	end if
	initialize the process
	end if
	return weights, K order, threshold error
	end
	on-line training
	Load weights, K order, threshold error, error signal
	while t < simulation time do
	Calculate the input and output value of each layer
	Calculate the errors between target and current value
	if $e_x < \text{threshold error}$
	return $k_1$
	else
	Update weights ec. Equation (10)
	Calculate the input and output value of each layer, ec.
	Equation (9)
	return $k_1$
	end

#### 4. Test Power System

Without loss of generality, the performance of our proposal is proved in an important benchmark of four machine and two area electric power system [1]. Although this system is not big, it presents an interesting and complex behavior for transient stability studies. The two areas are connected by a weak tie, this is an important case for studying the fundamental nature of inter-area oscillations and the inherent difficulty in tuning and controllers coordination.

##### 4.1. Case Base

A base analysis for different types of excitation control is presented in [1]. This power system has three rotor angle modes of oscillation. There is one inter-area mode of 0.55 Hz with generator 1 and 2 swinging against generators 3 and 4 of area 2. Two more are intermachine oscillation local modes, one of 1.09 Hz corresponds to area 1 and the second of 1.12 Hz is for area 2. These modes are determined only with one type of excitation control that changes if the operating condition varies or more dynamic components are involved.

In this analysis, each synchronous generator of Figure 4 is represented by the model Equation (1). Two loads are connected at bus 7 and 9. The initial conditions are based in data set reported in [1]. The active power injected by each generator:  $P_{G1} = P_{G2} = P_{G4} = 700$  MW and,  $P_{G3} = 719$  MW; terminal voltages:  $V_{tG1} = 1.03\angle 20.2$  pu,  $V_{tG2} = 1.01\angle 10.5$  pu,  $V_{tG3} = 1.03\angle -6.8$  pu,  $V_{tG4} = 1.01\angle -17.0$  pu. The initial conditions for state variables of each generator are obtained considering (1)–(4) using this information. The machine parameters are also available in [1] and used on this paper.

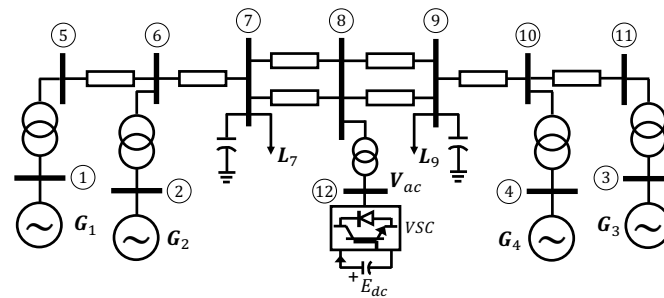


Figure 4. Four machine power system with StatCom at bus 8.

With this model representation and initial conditions, the system is exposed to a three-phase fault at different nodes with similar results, selecting node 7 on this section to illustrate the results.

The electrical grid without StatCom neither PSS exhibits an unstable performance when the fault is cleared after eight cycles, Figure 5. If the fault is cleared up to seven cycles a stable evolution is observed, but the oscillations have values far from the prefault condition, and with long duration. After 6 s the oscillations continue with very little damping. Figure 5 shows the angular difference between machines with generator number one as a reference, for eighth cycles (unstable operation) and six cycles (stable but oscillating operation). Additional damping required is evidenced. Similar behavior is observed in other system variables.

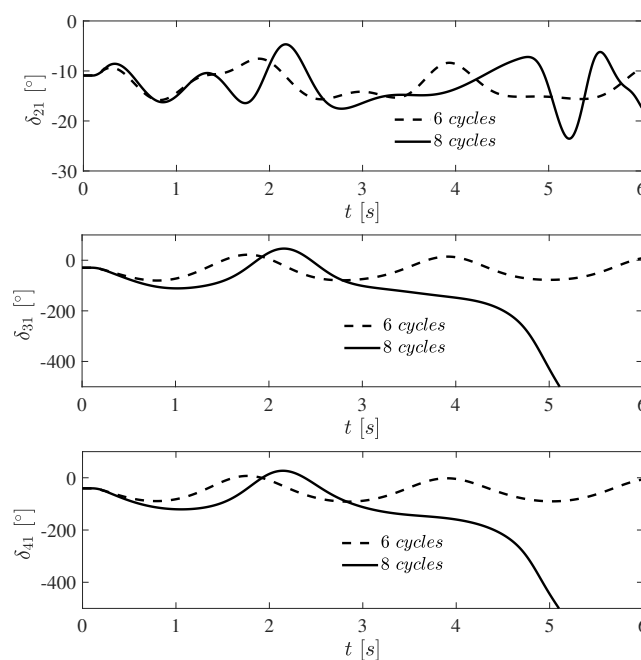
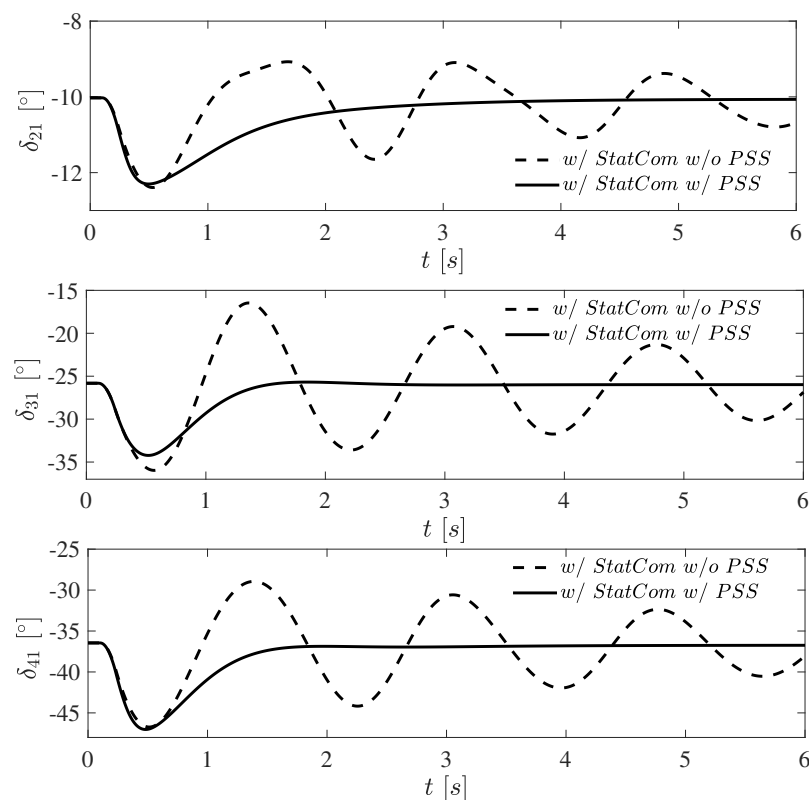


Figure 5. Angular difference of each machine with respect to number one, electrical grid without StatCom neither PSS.

#### 4.2. Case 1. Three-Phase Failure Cleared after Eight Cycles

This study considers a StatCom integrated to the power system at bus 8, as presented in Figure 4. Initially, the StatCom operation was forced to keep the system behavior very similar to one without StatCom and PSS. Therefore, the power flow solution is used to feed the calculation of initial conditions by the prefault situation of angles and voltage magnitude. At bus 8, the voltage magnitude is  $V_8 = 0.9556$  pu, close to the lower limit.

A three phase fault at 0.1 s is presented near to node 7 in one of the transmission lines 7–8. Several fault duration times were tested. Figures 6 and 7 exhibit the power system performance when the StatCom and PSS have a positive interaction. The fault is cleared after eight cycles, which was the fault duration for the power system to become unstable on the base case. There is a comparison using StatCom with and without PSS for making the system stable. The StatCom inclusion is not enough to improve the global power system damping, however, it diminishes the magnitude of the oscillations and improves the damping ratio respect to the system without controllers in the same period.



**Figure 6.** Angular difference of each machine with respect to number one, case 1: 8 cycles until the fault is cleared.

Figure 6 depicts the angular difference of each generator. The proposed control design methodology shows a positive interaction between controllers and the overshoot has an important reduction with and without the PSS, but the oscillations are eliminated in a fast way when PSS is included. Figure 7a presents the active power on the generator two and Figure 7b the voltage magnitude in PCC node where the StatCom is included.

Table 5 presents the main characteristics of transient response for case 1. Where the quantitative comparison is obtained in the case: (i) with StatCom and without PSS (wS/woPSS); and (ii) with StatCom and with PSS (wS/wPSS). The transient responses of the angular differences are improved with the correct coordination of controllers. In the case of  $\delta_{21}$  the settling time is diminished in about 80.5%, for the overshoot a marginal improves percent is obtained. However, the overall performance of the proposed technique

permits to attain a similar behavior in terms of overshoot, in some case better, but in all responses the settling time is drastically enhanced.

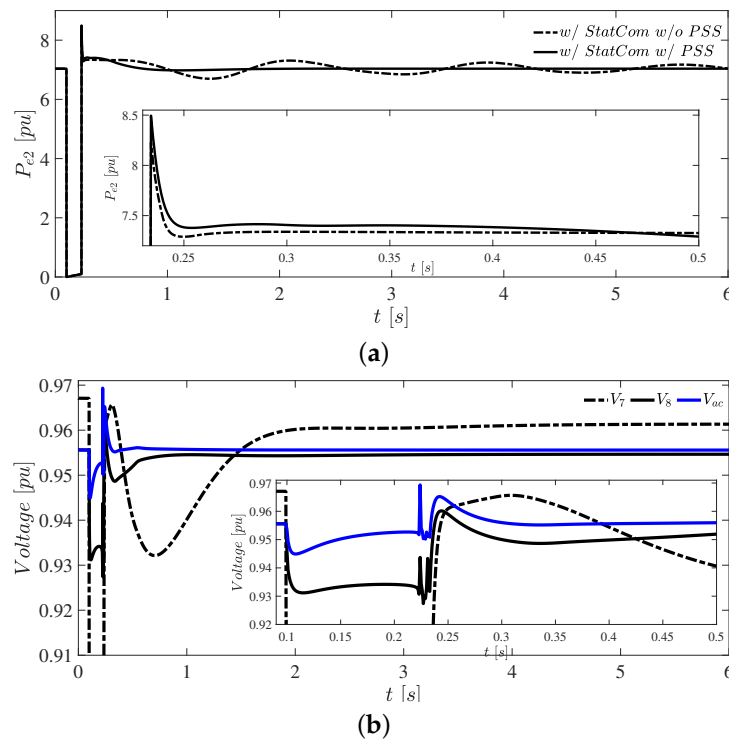


Figure 7. Case 1: (a) real power at generator 2; (b) voltage magnitude in bus of StatCom connection.

Table 5. Analysis in time domain of the responses for case 1.

Variable	Case	Rise Time	Settling Time	Overshoot	Peak Time
$\delta_{21}$	wS/woPSS	0.0802	14.4562	2.3927	0.5300
	wS/wPSS	0.0198	3.8236	2.2998	0.4960
$\delta_{31}$	wS/woPSS	0.0515	16.1978	10.1564	0.5670
	wS/wPSS	0.0205	2.2131	8.5395	0.5180
$\delta_{41}$	wS/woPSS	0.0571	15.7923	10.2529	0.5120
	wS/wPSS	0.0238	2.8591	10.3163	0.4820
$P_{e2}$	wS/woPSS	0.00054	4.0704	1.2251	0.2340
	wS/wPSS	0.00052	0.5917	1.4949	0.2340

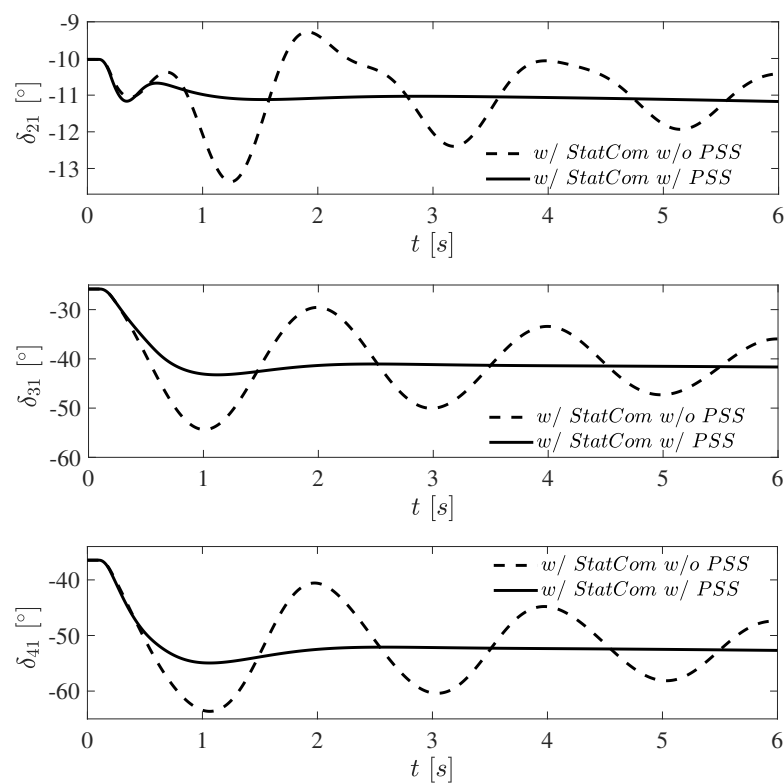
The settling time is improved with the following percentages; for  $\delta_{31}$ , 86.3%; for  $\delta_{41}$ , 81.9%, and  $P_{e2}$ , 85.5%, which is concentrated in Table 6. The rise time and peak time are similar for both controller's tuning. Like the previous dynamic performance of the power system, for the case 2, also the transient response features are determined, Table 6. Now, the proposed adaptive strategy has impacted in two main features in time domain transient response. Both settling time and overshoot are clearly enhanced by the proposed control coordination scheme. The following improvement values are attained:  $\delta_{21}$ , 83%;  $\delta_{31}$ , 87.5%;  $\delta_{41}$ , 86%, and  $P_{e2}$  in 85%. In Table 6, the results are presented. It is evident the correct performance of the proposed algorithm to diminish the exhibited low frequency oscillations in a faster way. Additionally, the percent that diminishes the overshoot in this case is:  $\delta_{21}$ , 65%;  $\delta_{31}$ , 70%;  $\delta_{41}$ , 79%, and  $P_{e2}$  in 43.3%.

**Table 6.** Analysis in time domain of the responses for case 2.

Variable	Case	Rise Time	Settling Time	Overshoot	Peak Time
$\delta_{21}$	wS/woPSS	0.1568	9.7201	2.1921	1.2450
	wS/wPSS	0.1339	1.6374	0.4907	0.3415
$\delta_{31}$	wS/woPSS	0.3151	17.6893	12.6784	1.0090
	wS/wPSS	0.4666	2.2153	1.5931	1.1230
$\delta_{41}$	wS/woPSS	0.3149	14.7150	10.9615	1.0640
	wS/wPSS	0.3860	2.0571	2.2949	1.0620
$P_{e2}$	wS/woPSS	0.0026	4.9918	0.4435	0.8310
	wS/wPSS	0.0019	0.7363	0.2515	0.7930

#### 4.3. Case 2. Three-Phase Failure with Line Out of Service after Eight Cycles

In contrast to case 1, now the postfault condition is with one of the parallel transmission lines 7–8 out of service after the fault is cleared. The fault with six cycles of duration is presented between buses 7–8, close to node 7. The proposed methodology has a behavior similar to case 1, Figures 8 and 9.

**Figure 8.** Angular difference of each machine with respect to number one, case 2.

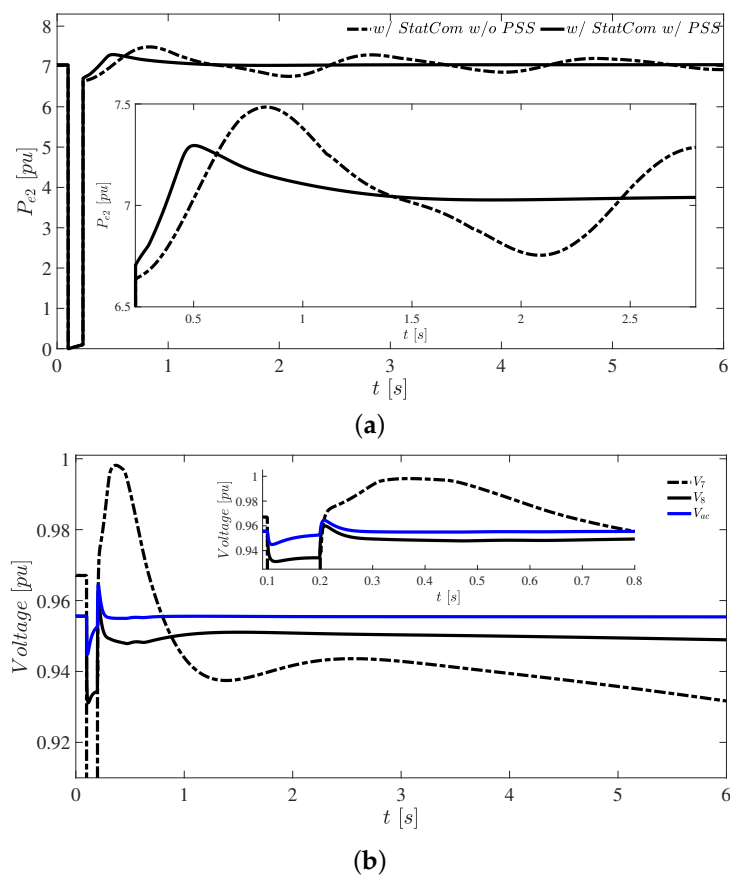
The angular difference of machines respect to number one are presented in Figure 8. The overshoot after the fault is released is bounded and the oscillations of internal machine angle exhibit fast transient respond reaching a new value in steady state. The final condition is due to a new electrical grid topology with one transmission line out of service.

Figure 9a reveals the active power injected by the generator 2. With improved control design stage and dynamic gains, the controllers are adapted to the new power system

condition or perturbation presented. The power oscillations are diminished after one second. With only StatCom the oscillations are diminished with low magnitude.

In Figure 9b some voltage magnitudes are presented. At node 8 where StatCom is connected the voltage magnitude returns to the set point, however, it is close to low voltage limit. In the case of faulted node 7, the system tries to return a stable condition, but the voltage is below low limit. Thus, an action of secondary control loop is required to reach the new steady state condition where all variables should be within physical limits.

The evolution of the gains is exhibited in Figure 10a, the updated values allow to get the best performance. All results are in accordance with the expected values of the power system with improved damping ratio due to the design procedure and the inclusion of some dynamic gains. Additionally, the performance of these gains in case 2 is presented in Figure 10a, the initial conditions are equal for both study cases but have different dynamic evolution.



**Figure 9.** Case 2: (a) real power at generator 2; (b) voltage magnitude in bus of StatCom connection.

In Figure 10b, the control signals for the StatCom are displayed. The calculated gains are meant to get a fast response with limited overshoot, after the transient period both control signals attain a new steady state condition. Similar behavior for both cases is exhibited in these signals.

The deviation respect to initial values is small, and with very fast response (less than one second).

Cases 1 and 2 demonstrate the improved dynamic performance that the power system exhibits by using the variables of this section. The simulation results indicate that critical clearing time has been improved widely. Under this scenario the presented results illustrate the system response when the fault is cleared after six cycles. The prefault and postfault condition are the same.

Then, without loss of generality it is possible to extend our methodology in electric power system with more generators, different FACTS devices, generation plants and emerging technologies. Under these new conditions some minor considerations must be included in B-Spline scheme for on line operation.

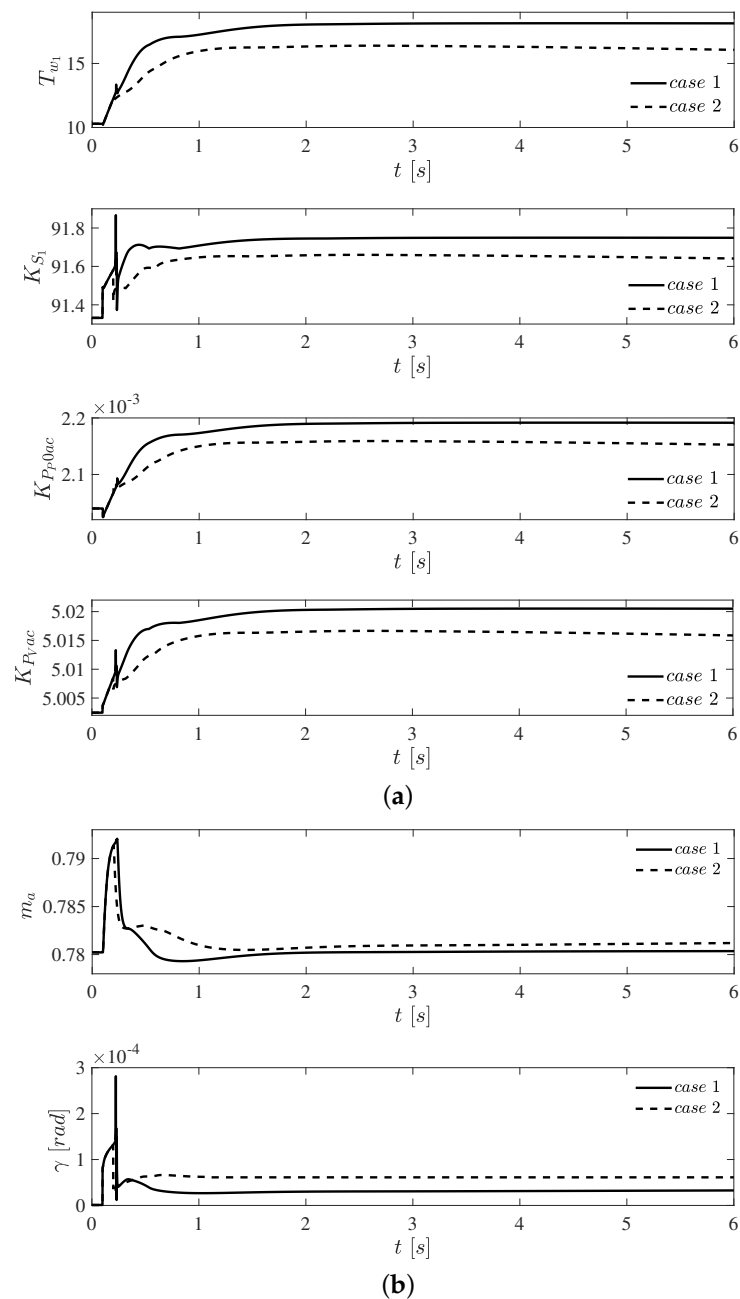


Figure 10. (a) Evolution of dynamic gains and; (b) Control signals for the StatCom.

### 5. Conclusions

The proposed design methodology includes a complete non-linear representation of large-scale power systems for transient stability studies. Three-phase failure is presented to validate stability. On the base case, the angular difference of the machines is not ensured when failure is released after 8 cycles. The power system presents enhanced dynamic performance when StatCom and PSS are included. The PSS and the StatCom controllers are simultaneously tuned using B-Spline for gain definition, and using typical known values for each gain. Model uncertainties are not included in the design stage because



they are considered on the gains updating task, which is performed in each sample time, avoiding model and parameter dependency. The control design stage allows good system performance under a specific operating point but also with other operating conditions or topologies. Moreover, the new proposed technique can be extended to other complex multimachine power systems with several adaptive dynamic controllers.

**Author Contributions:** Conceptualization, R.T.-O.; Data curation, O.A.-M.; Formal analysis, F.B.-C.; Investigation, R.T.-O.; Methodology, R.T.-O., F.B.-C. and A.V.-G.; Supervision, F.B.-C. and A.V.-G.; Validation, O.A.-M.; Writing—original draft, R.T.-O.; Writing—review—editing, A.V.-G. All authors have read and agreed to the published version of the manuscript.

**Funding:** This research received no external funding.

**Institutional Review Board Statement:** Not applicable.

**Informed Consent Statement:** Not applicable.

**Data Availability Statement:** No new data were created or analyzed in this study. Data sharing is not applicable to this article.

**Acknowledgments:** R.T.-O. and O.A.-M. thank to the CONACYT-SENER-SUSTENTABILIDAD ENERGÉTICA the support to develop this work under grant CEMIE-REDES PE-A-21. A.V.-G. thanks Universidad Panamericana the support to develop this work. R.T.-O. thanks to the Programa de Apoyo a Proyectos de Investigación e Innovación Tecnológica (PAPIIT) de la UNAM. Con clave UNAM-DGAPA-PAPIIT- IA106920.

**Conflicts of Interest:** The authors declare no conflict of interest.

## References

1. Kundur, P.; Balu, N.; Lauby, M. *Power System Stability and Control*; McGraw-Hill Education: New York, NY USA, 1994; Volume 7.
2. Kang, R.D.; Martinez, E.A.; Viveros, E.C. Coordinated tuning of power system controllers using parallel genetic algorithms. *Electr. Power Syst. Res.* **2021**, *190*, 106628. [[CrossRef](#)]
3. Liu, M.; Bizzarri, F.; Brambilla, A.M.; Milano, F. On the Impact of the Dead-Band of Power System Stabilizers and Frequency Regulation on Power System Stability. *IEEE Trans. Power Syst.* **2019**, *34*, 3977–3979. [[CrossRef](#)]
4. Rana, M.J.; Shahriar, M.S.; Shafiullah, M. Levenberg–Marquardt neural network to estimate UPFC-coordinated PSS parameters to enhance power system stability. *Neural Comput. Appl.* **2019**, *31*, 1237–1248. [[CrossRef](#)]
5. Pandey, R.K.; Gupta, D.K. Integrated multi-stage LQR power oscillation damping FACTS controller. *CSEE J. Power Energy Syst.* **2018**, *4*, 83–91. [[CrossRef](#)]
6. Bayatloo, F.; Bozorgi-Amiri, A. A novel optimization model for dynamic power grid design and expansion planning considering renewable resources. *J. Clean. Prod.* **2019**, *229*, 1319–1334. [[CrossRef](#)]
7. Xu, T.; Birchfield, A.B.; Overbye, T.J. Modeling, tuning, and validating system dynamics in synthetic electric grids. *IEEE Trans. Power Syst.* **2018**, *33*, 6501–6509. [[CrossRef](#)]
8. Rimorov, D.; Kamwa, I.; Joós, G. Model-based tuning approach for multi-band power system stabilisers PSS4B using an improved modal performance index. *IET Gener. Transm. Distrib.* **2015**, *9*, 2135–2143. [[CrossRef](#)]
9. Talaq, J. Optimal power system stabilizers for multi machine systems. *Int. J. Electr. Power Energy Syst.* **2012**, *43*, 793–803. [[CrossRef](#)]
10. Salgotra, A.; Pan, S. Model based PI power system stabilizer design for damping low frequency oscillations in power systems. *ISA Trans.* **2018**, *76*, 110–121. [[CrossRef](#)]
11. Gomes, S., Jr.; Guimarães, C.; Martins, N.; Taranto, G. Damped Nyquist Plot for a pole placement design of power system stabilizers. *Electr. Power Syst. Res.* **2018**, *158*, 158–169. [[CrossRef](#)]
12. Liu, X.; Han, Y. Decentralized multi-machine power system excitation control using continuous higher-order sliding mode technique. *Int. J. Electr. Power Energy Syst.* **2016**, *82*, 76–86. [[CrossRef](#)]
13. Patel, A.; Ghosh, S.; Folly, K.A. Inter-area oscillation damping with non-synchronised wide-area power system stabiliser. *IET Gener. Transm. Distrib.* **2018**, *12*, 3070–3078. [[CrossRef](#)]
14. Sands, T. Development of Deterministic Artificial Intelligence for Unmanned Underwater Vehicles (UUV). *J. Mar. Sci. Eng.* **2020**, *8*, 578. [[CrossRef](#)]
15. Cooper, M.; Heidlauf, P. Nonlinear feed forward control of a perturbed satellite using extended least squares adaptation and a luenberger observer. *J. Aeronaut. Astronaut. Eng.* **2018**, *7*, 1–7. [[CrossRef](#)]
16. Shi, Y.; Sarlioglu, B.; Lorenz, R.D. Real-time loss minimizing control of induction machines for dynamic load profiles under deadbeat-direct torque and flux control. *IEEE Trans. Ind. Appl.* **2021**, *1*, 1–9.

17. Yao, W.; Jiang, L.; Wen, J.; Wu, Q.; Cheng, S. Wide-area damping controller for power system interarea oscillations: A networked predictive control approach. *IEEE Trans. Control Syst. Technol.* **2014**, *23*, 27–36. [[CrossRef](#)]
18. Farahani, M.; Ganjefar, S. Intelligent power system stabilizer design using adaptive fuzzy sliding mode controller. *Neurocomputing* **2017**, *226*, 135–144. [[CrossRef](#)]
19. Yousefian, R.; Kamalasadani, S. A Lyapunov function based optimal hybrid power system controller for improved transient stability. *Electr. Power Syst. Res.* **2016**, *137*, 6–15. [[CrossRef](#)]
20. Ray, P.K.; Paital, S.R.; Mohanty, A.; Eddy, F.Y.; Gooi, H.B. A robust power system stabilizer for enhancement of stability in power system using adaptive fuzzy sliding mode control. *Appl. Soft Comput.* **2018**, *73*, 471–481. [[CrossRef](#)]
21. Afzalan, E.; Joorabian, M. Analysis of the simultaneous coordinated design of STATCOM-based damping stabilizers and PSS in a multi-machine power system using the seeker optimization algorithm. *Int. J. Electr. Power Energy Syst.* **2013**, *53*, 1003–1017. [[CrossRef](#)]
22. Wang, S.K. Coordinated parameter design of power system stabilizers and static synchronous compensator using gradual hybrid differential evaluation. *Int. J. Electr. Power Energy Syst.* **2016**, *81*, 165–174. [[CrossRef](#)]
23. Al-Ismael, F.; Hassan, M.; Abido, M. RTDS implementation of STATCOM-based power system stabilizers. *Can. J. Electr. Comput. Eng.* **2014**, *37*, 48–56. [[CrossRef](#)]
24. Padiyar, K. *Power System Dynamics: Stability and Control*; Anshan: Kent, UK, 2004.
25. Castro, L.M.; Acha, E.; Fuerte-Esquivel, C.R. A novel STATCOM model for dynamic power system simulations. *IEEE Trans. Power Syst.* **2013**, *28*, 3145–3154. [[CrossRef](#)]
26. Brown, M.; Harris, C.J. *Adaptive B-Spline Networks, Neurofuzzy Adaptive Modelling and Control*; Prentice Hall: New York, NY, USA, 1994.
27. Toshniwal, D.; Speleers, H.; Hiemstra, R.R.; Manni, C.; Hughes, T.J. Multi-degree B-splines: Algorithmic computation and properties. *Comput. Aided Geom. Des.* **2020**, *76*, 101792. [[CrossRef](#)]
28. Tapia, R.; Aguilar, O.; Minor, H.; Santiago, C. Power system stabilizer and secondary voltage regulator tuning for multi-machine power systems. *Electr. Power Components Syst.* **2012**, *40*, 1751–1767. [[CrossRef](#)]
29. Beltran-Carbajal, F.; Tapia-Olvera, R.; Lopez-Garcia, I.; Guillen, D. Adaptive dynamical tracking control under uncertainty of shunt DC motors. *Electr. Power Syst. Res.* **2018**, *164*, 70–78. [[CrossRef](#)]